1. OBJECTIVES

Spinal cord sympathetic preganglionic neurons (**SPNs**) are the final arbiters of CNS sympathetic output. SPN axons that project to paravertebral ganglia branch to issue divergent multisegmental projections on postganglionic neurons in paravertebral sympathetic chain ganglia (***Fig 1***). Divergence provides a mechanism for amplification of CNS sympathetic commands to the numerically much greater postganglionic neurons (~200:1 in human & 14:1 in mouse) [1]. It is assumed that "preganglionic signals are distributed widely through paravertebral ganglia with little modification" [2] but studies on spike conduction across multisegmental branch points were based on recorded synaptic actions in the isolated *ex vivo* guinea pig thoracic chain at room temperature [3-7] where large increases in spike amplitude and width may ensure a high safety factor for branch point conduction [8, 9]. Conversely, increasing temperature (**T°**) promotes conduction failures, particularly when above core body T° [8, 9]. It is likely that SPN branch point conduction is also T°-sensitive.

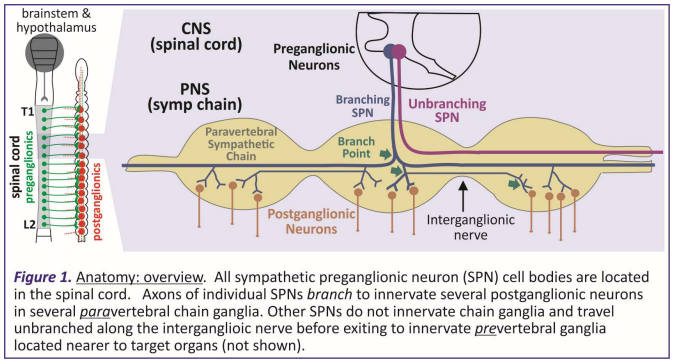

Figure 1. Anatomy: overview. All sympathetic preganglionic neuron (SPN) cell bodies are located in the spinal cord. Axons of individual SPNs *branch* to innervate several postganglionic neurons in several *para*vertebral chain ganglia. Other SPNs do not innervate chain ganglia and travel unbranched along the interganglioic nerve before exiting to innervate *pre*vertebral ganglia located nearer to target organs (not shown).

In somatosensory systems, branch points provide a nodal site for modulatory control of conduction [10-13]. Extrasynaptic α_5-containing $GABA_A$ receptors (**$GABA_ARs$**) are implicated [12-14]. SPNs, too, express constitutively-active α_5-$GABA_ARs$ [15]. If expressed at axonal branch points, the modifiability may similarly control divergence and hence response amplification to postganglionic neurons. After nerve or spinal cord injury (**SCI**) there is circuit hyperexcitability [16-20] via transporter-dependent loss of GABAergic inhibitory effects due to depolarizing changes in chloride reversal ($\mathbf{E_{Cl}}$) [21, 22]. Analogously, plasticity in SPN α_5-$GABA_AR$ function after SCI may contribute to the emergent autonomic dysfunction.

We recorded from diverging SPN axons across ganglia in the adult mouse *ex vivo* thoracic *paravertebral* chain following stimulation of attached SPNs in spinal roots to look for modulation of SPN spike propagation beyond the spike-initiating initial axon segment [23]. We obtained convincing evidence of alterations in conduction that was dependent on; ①number of traversed chain ganglia, ②temperature (**T°**), ③constitutive $GABA_AR$ activity, and ④stimulus frequency. Dye filling of SPN projections from an individual root showed extensive rostrocaudal axonal divergence of component SPNs. In sum, the assumption of signal distribution "*with little modification*" was not supported, introducing SPN axonal divergence as a modifiable output stage in sympathetic gain control. We hypothesize that spike conduction failures and modulation of conduction occurs at axonal branch points via physiologically regulatable mechanisms. To strengthen the hypothesis, proposed aims below compare actions on SPN paravertebral branching axons to SPN unbranching axons that travel through the chain to project to *prevertebral* ganglia in the splanchnic nerve (***Fig 2B***).

[SA1 HYPOTHESIS] Branch point conduction is sensitive to observed changes in body T^0.

Many SCI individuals have thermoregulatory dysfunction [24-27]. As even small changes above normal body T° can compromise spike conduction [9] the SCI population may be particularly vulnerable. We will test the effect of ΔT° on conduction block across segmental branch points over

a range of T° consistent with the physiological range of hypo- or hyperthermia seen after SCI [24-27] and the broader ΔT° seen during life-threatening hypo- or hyperthermia (32-40°C) [28-30].

[SA2 HYPOTHESIS] Conduction across SPN branch points is modulated by $GABA_AR$s.

Modulation via presynaptic axonal α_5-$GABA_AR$s would provide an unrecognized mechanism for control of response amplification of rostrocaudal actions. Such control at the CNS-PNS interface enables access to humoral factors that have known actions on α_5-$GABA_AR$s [31-35]. This occurs via systemic changes in constitutively active $GABA_AR$s by endogenous allosteric modulation and by Cl^- transporter mediated changes in Cl^- reversal potential ($\mathbf{E_{Cl}}$).

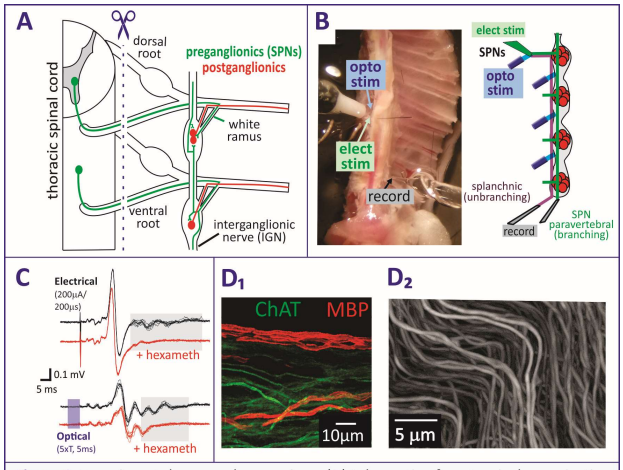

Figure 2. Experimental approach: overview. **(A)** Schematic of anatomical organization showing approach enabling selective activation of preganglionics via stimulation of the ventral root. **(B)**Picture of the adult *ex vivo* prep and adjacent schematic to show experimental configuration including optogenetic recruitment of SPN from ventral root (e.g. ChAT-CHR2 mice). **(C)** Direct axon volley following electrical or optical SPN recruited axons can be isolated from postganglionic axons following block of nicotinic synaptically-evoked response with hexamethonium. **(D)** SPN axon composition is dominated by small-diameter unmyelinated axons. **(D_1)** ChAT::YFP mouse showing unmyelinated (green) and myelinated SPN axons in white ramus identified with myelin basic protein (MBP - red). **(D_2)** Image enhanced confocal scan of white ramus showing unmyelinated axons.

[SA1 & SA2 SPINAL CORD INJURY] As SCI is a life-altering neurologic trauma with impaired sympathetic autonomic control can impact body temperature ($\mathbf{T°_{core}}$) [24-27] and can cause changes in Cl^- transport across $GABA_AR$s [21, 22], results obtained in **[SA1]** & **[SA2]** will be compared to those seen after T2 thoracic SCI at acute (1-3 days) and chronic (4-6 weeks) time points. As there is also evidence of circadian regulation of Cl^- transport [36], and SPNs receive direct hypothalamic projections under circadian control, SCI may lead to dysregulation in circadian E_{Cl} impacting $GABA_AR$ modulation in spike conduction across branch points.

[SA3 HYPOTHESIS] Branching axons are uniquely prone to activity-dependent conduction changes.

Almost all (99%) of mouse SPN axons are unmyelinated with mean diameter of 0.4 μm and branching diameters can be as low as 0.1 μm [37]. Such small axons would be expected to undergo considerable activity-dependent hyperpolarization, conduction slowing and block [38, 39]. Frequency-dependent changes in conduction across branch points have not been examined in SPNs innervating thoracic paravertebral ganglia. Their small diameter may make them particularly sensitive to Na^+ channel inactivation [40] and hyperpolarization by a $[Na^+]_i$ sensitive metabolic rheostat provided by the α_3-Na^+/K^+ pump that tracks activity history [41]. α_3-Na pumps are ubiquitously expressed in neurons [42] and may play a prominent role in in regulating autonomic activity dynamics [43].

[SA4] Modeling approaches to explore interacting factors controlling axonal conduction.

As intra-axonal recordings are essentially impossible due to small axon size, modeling studies will provide critical putative mechanistic insight into observed population responses recorded extracellularly. In addition to exploring the impact of T° and $GABA_AR$-E_{Cl}, multiple geometric and biophysical factors – often not experimentally manipulatable – influence whether action potentials faithfully propagate through SPN branch points or fail. Some of these factors interact in counter-intuitive ways. We will use computational ensemble modeling to examine the interacting factors controlling autonomic axonal conduction.

2. RATIONALE AND SIGNIFICANCE

RATIONALE. This proposal explores a conceptually novel mechanism of CNS-PNS gain control in a little explored but physiologically critical area in vertebrate neuroscience: the CNS sympathetic output stage. SPNs control paravertebral postganglionic systems along thoracic sympathetic chain ganglia that prominently participate in regulating blood flow to distributed organ systems such as muscle and skin [44, 45]. We developed an *ex vivo* adult mouse that enabled the first whole-cell recordings in this region, providing accurate cellular characterization, and paired this with computational modeling of thoracic chain postganglionic neurons. While thoracic postganglionic neuronal populations are comprised of 5 genetically distinct adrenergic subpopulations [46], little is known about their recruitment by SPNs, themselves comprising a genetically heterogeneous population that is almost as neurochemically diverse as the hypothalamus [47]. Recent technical elaborations [48] now enable exploration of SPN output control by elements that occur beyond the centrally encoded SPN firing at the axonal initial segment.

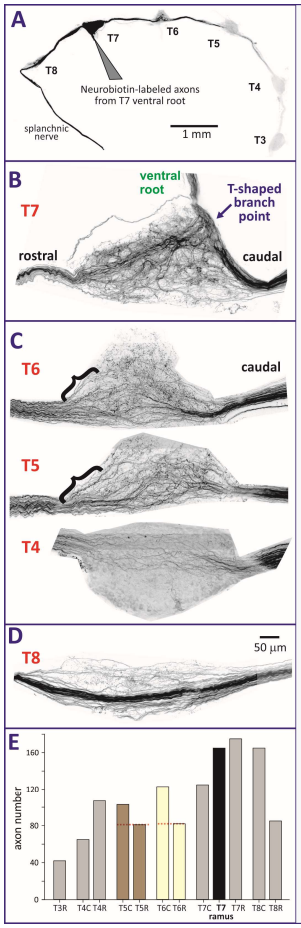

Figure 3. Rostrocaudal divergence of SPN projections in sympathetic chain arising from T7 spinal segment. **(A)** T7 SPN axons were labeled with Neurobiotin after diffusion from the T7 ventral root. Labeling is seen along T3-T8 chain ganglia and in the splanchnic nerve *[T9-12 ganglia are missing]*. **(B)** T7 SPN axons form a 'T' shaped branch point junction. Many axons project into the ganglia neuropil to form synapses (black dots) but then reassemble back into tracts as part of the rostrally and caudally-projecting interganglionic nerves. **(C)** Many T6 and T5 axons issue collaterals to form synapses before reassembling (see parentheses) for further rostral projections in respective interganglionic nerves. Far fewer axons remain at T4. **(D)** Most SPN axons that travel caudally are unbranching and form the splanchnic nerve that predominantly innervate the celiac ganglion. **(E)** Counts of of Neurobiotin labeled axon numbers in the T7 ramus and in interganglionic nerves protecting rostrally and caudally between T3 and T8 sympathetic ganglia. Note that as axons travel caudally from T7 caudally, more axons exit both T6 and T5 ganglia than enter (see dotted horizontal lines in red). This suggests that axons branching within the sympathetic chain to innervate postganglionic neurons do not reform but rather continue projecting as two independent sister branches.

Consideration of SPN axonal branch points as a nodal site for modulatory control of sympathetic output strength has been ignored. We assert that control of conduction along SPN multisegmental axonal branches is an overlooked but important physiologically modifiable presynaptic feature in output control. This study focuses on SPNs innervating paravertebral thoracic chain ganglia. The circuit studied is intimately involved in modulation of stress, metabolism, blood distribution and thermoregulation [44]. The intention of this proposal is to demonstrate that conduction across SPN branch points is physiologically relevant and modifiable. Regarding clinical relevance, our emphasis here is to establish putative mechanisms and their relevance to SCI to enable subsequent strategic emphasis on validity *in vivo*.

Factors that may control spike conduction across axonal branch points. Geometrical factors of the primary axon and its branching collaterals dictate the success of spike propagation. For example, if the combined cross-sectional area of daughter branches is greater than the cross-sectional area of the parent axon, the lower input impedance creates a current sink ahead of a propagating spike that can reduce spike amplitude and cause conduction failure [49]. These details will be explored in a recently developed model constructed from anatomic data. Factors that affect spike conduction include T°, activity dependence, the presence of various ion channels [49, 50] and extra-synaptic $GABA_AR$s [12, 13]. **(a) Temperature.** Branch point failure has not been considered a feature of the SPN projections [2]. However, this was based on recordings of

multisegmental actions in the isolated *ex vivo* guinea pig thoracic chain at room T° [3-7]. Conduction failures are more common at increasing T° with unmyelinated axons being particularly sensitive [8, 9, 49]. A T°-dependent reduction in spike amplitude and width may contribute to conduction failure at higher T° [8] while lower T° likely reduces conduction failures by increasing spike amplitude and duration, as may also be accomplished with block of K^+ currents [51, 52]. As SPNs are predominantly unmyelinated [37] (***Fig 2D & 3***) and show variations in diameter and branching, reliability of conduction at their branch points would also be expected to be T°-sensitive [52-54] and modifiable by hypo- and hyperthermia [24-30]. **(b) Activity-dependent actions.** It is thought that "preganglionic signals are distributed widely through paravertebral ganglia with little modification" [2]. Yet elsewhere, axonal branch points are prone to conduction failure and are under modulatory control [49, 55]. Almost all (99%) mouse paravertebral SPN axons are unmyelinated with mean diameter of 0.4 µm and branch diameters can be as low as 0.1 µm [37]. One prominent feature of unmyelinated axons is frequency-dependent hyperpolarization, conduction slowing and block [38, 40, 56-58]. In the absence of ability to record from individual axons, differences in population changes in activity coupled with individual axonal modeling strategies may deepen our understanding of the rules governing population circuit dynamics. This includes: (a) frequency- and history-dependent mechanisms, (b) SPN-postganglionic control of spike conduction, including divergence across multiple branch points, and (c) recruitment of SPNs driven by descending systems that include persistent actions over long periods at low frequency, as in the baroreflex [44]. However, higher frequencies are also seen during excessive physiological stress and genetically identifiable CART-expressing SPNs may represent a unique group of accessory SPNs recruited during conditions of stress [59, 60]. Spike frequency and/or bursting within a given axon may be tuned with a metabolic rheostat provided by the α_3-Na^+/K^+ pump that retains activity history and are ubiquitously expressed in neurons [41, 42]. α_3-Na pumps have low Na^+ affinity, are weakly active at rest, and can act as a sensor for activity-dependent rises in Na^+ [42] and thus respond dynamically to Na^+ changes of prolonged firing with hyperpolarization that

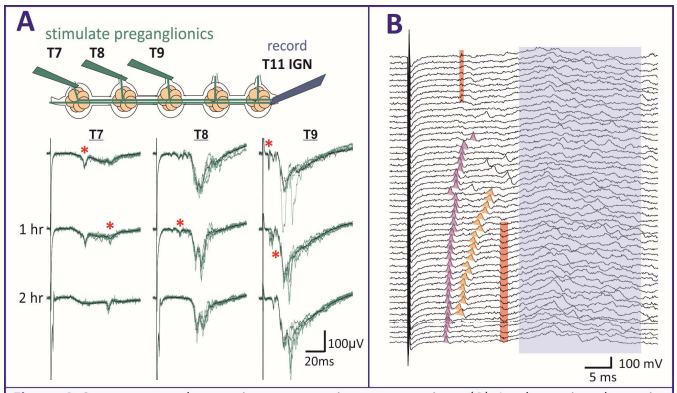

Figure 4. Spontaneous changes in axon recruitment over time. **(A)** As shown in schematic, electrical stimulation was undertaken at 3 different ventral roots while recording past the T11 ganglion in the interganglion nerve (IGN). Evoked responses are larger when stimulation site is closer than recording site.Stimuli were delivered 1/30s. Red astericks showing incidences of spontaneous emergence or loss of conduction over the course of 2 hours. **(B)** Raster of individual records of the evoked responses following stimulation of the T9 ventral root at 1 min intervals for 45 min. Note two larger early units emerge and are recruited at progresivey earlier latency, consistent with increased security of conduction across branch ponta (**purple** and **orange** underlining). Other emergent or lost events are boxed in **pink**. Note also the high variability in the population response of later arriving and much more numerous unmyelinated axons (**blue** shading) precludes individual assessment but can be quantified by comparing changes in the rectified integral. Experiments were undertaken following block of synaptic transmission with hexamethonium. Stimulation in all panels was at 200 µA, 200 µs.

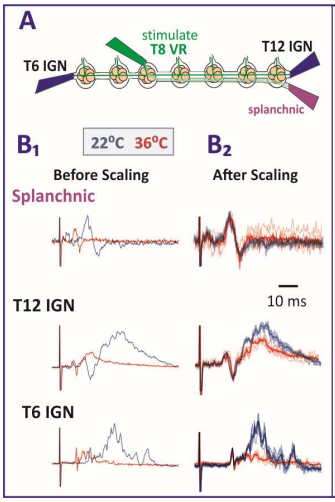

Figure 5. Preferential temperature sensitivity of spike propagation across branching SPN axons. **(A)** Schematic of experiment showing T8 ventral root stimulation while recording branching axons in rostral T6 and caudal T12 interganglionic nerve (IGN) as well non-branching axons in the adjacent splanchnic nerve. **(B_1)** Overlay of evoked average responses at 22° and 36°C to demonstrate strong T° effect on latency and amplitude of recruited spikes. **(B_2)** 36°C responses are time-amplitude expanded to best fit 22°C response. Note that splanchnic response fits well while there is some loss in recruitment of longer-latency unmyelinated axon recruitment in branching axons in the IGN.

can last many seconds [41, 45, 61]. In comparison, the primary α_1-Na pumps are increased when Na^+ ions accumulate intracellularly following intense firing [42]. A role for axonal α_3-Na pumps in regulating frequency and spike conduction in branching SPNs has not been considered. **(c) Extrasynaptic $GABA_AR$s.** $GABA_AR$s can control conduction across primary afferent branch points [49] and extra-synaptic $GABA_A$ receptors [10] have clear actions at branch points [13, 62]. Block of α_5-containing $GABA_A$ receptors (with L655,708, gabazine or bicuculline) *hyperpolarized* proprioceptors [13]. With respect to sympathetic chain ganglia, early studies observed putative GABA-modulated transmission [63-68] best explained by control of spike conduction in the presynaptic SPNs [68]. A preganglionic (SPN) locus is strongly supported by recent RNAseq-based data showing a lack of expressed $GABA_AR$s in postsynaptic postganglionic neurons [46]. The physiological significance of $GABA_AR$s in SPN axons within sympathetic ganglia in the absence of GABAergic neurons was hard to understand, and the field of inquiry was abandoned ~40 years ago [63, 68, 69]. More recently, intrasomatic recordings from SPNs observed membrane *depolarization* following block of $GABA_AR$s with bicuculline and not gabazine, consistent with actions on extrasynaptic α_5-$GABA_AR$s (confirmed with PCR) [70]. Receptor activation was insensitive to TTX (unlike that seen for myelinated afferents [13]), and the lack of gabazine action and additional pharmacology supported the presence of constitutively active $\alpha_5\delta_2$-$GABA_AR$s [70-72]. If these constitutively active $GABA_AR$s are also expressed in SPN axons projecting to postganglionic neurons, no GABA would be required, and the previously inexplicable early observations seen with $GABA_AR$ could be due to block of constitutively active $\alpha_5\delta_2$-$GABA_AR$s. We obtained preliminary evidence of constitutively active $GABA_AR$s on SPN axons (***Fig 6A***). Whether their actions are depolarizing [13, 14] or hyperpolarizing depends on activities in Cl^- transporters that set Cl^- reversal potential ($\mathbf{E_{Cl}}$) and remains to be determined. Importantly, by having axonal projections outside the CNS, their possible control by humoral endogenous allosteric modulators may transform our understanding of autonomic gain control at the CNS-PNS interface and introduce α_5-$GABA_AR$s as a novel pharmacologic target for the management of sympathetic dysfunction after SCI.

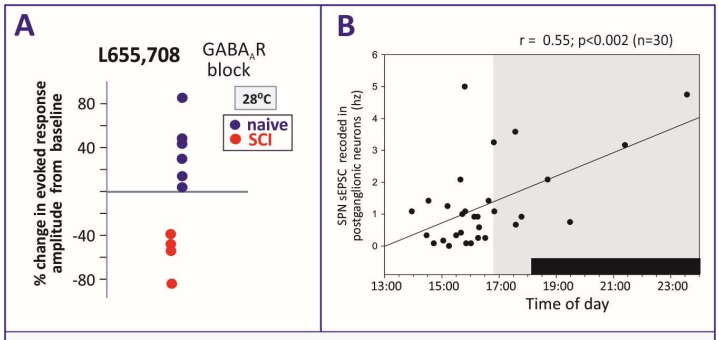

Figure 6. SCI-induced and circadian changes in SPN function may associate with alteration in Cl^- transporter function. **(A)** Experiments to assess change in conduction in branching axons recorded 3+ segments away. The inverse agonist L655, 708 blocks α5-containing $GABA_AR$s in the absence of GABA as an agonist. This is consistent with constitutively active $GABA_AR$s having inhibitory control over population spike propagation across branch points (n=6 mice). In contrast application of L655, 708 led in mice >3 weeks after T2 SCI contusion led to an inhibitory action (n=4 mice). **(B)** In a separate study spontaneous EPSC activity was recorded from postganglionic neurons. Under the assumption that there is circadian variation signal transduction pathways that reciprocally modulate KCC2 ansd NKCC1, constitutive $GABA_AR$ activity at time of E_{Cl} being depolarizing may lead to increased spontaneous synaptic transmission may precede and be elevated during the nocturnal active period. Consistent with this there is a moderate positive correlation between time of day and frequency of spontaneous EPSCs.

(d) Physiological mechanisms controlling KCC2 and NKCC1. The cation-chloride cotransporters KCC2 and NKCC1 regulate neuronal Cl^- levels in CNS neurons [18, 73]. They are homeostatically controlled by WNK-SPAK kinase induced phosphorylation which reciprocally down-regulates KCC2 and up-regulates NKCC1, leading to reduced Cl^- extrusion and increased Cl^- influx, respectively [18, 74-77]. This pathway is modulated by $[Cl^-]_i$ such that increases in $[Cl^-]_i$ as may occur after prolonged $GABA_AR$ activation, turn off the WNK-SPAK pathway, leading to increased membrane KCC2 expression, whereas $GABA_AR$ blockade leads to WNK-SPAK kinase activation and Cl^- extrusion. KCC2 and NKCC1 play an important role in the regulation of afferent-evoked responses. After SCI, KCC2 expression is reduced [21], changing E_{Cl} to more

positive values and causing $GABA_AR$ activation to drive development of pain sensitization. Importantly, changes occur rapidly [22], and KCC2 downregulation occurs rapidly through activation of signal transduction pathways that likely alter protein trafficking in membrane stabilization [78-80].

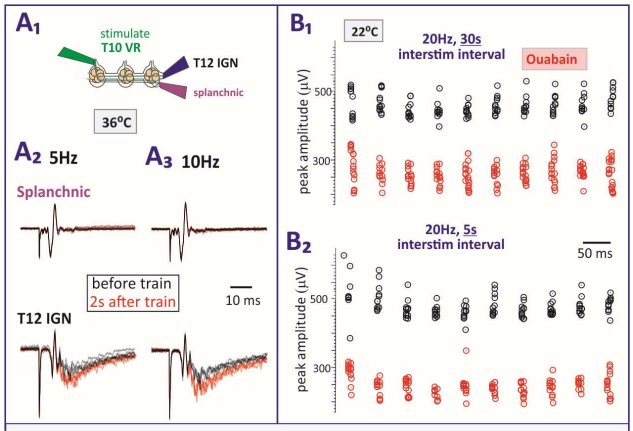

Figure 7. Frequency dependent modulation of conduction. **(A)** Preferential frequency-dependent sensitivity of spike propagation across branching SPN axons. **(A_1)** Effects of response of 5 pulses at 5Hz **(A_2)** or 10Hz **(A_3)** on axon recruitment at 36°C . SPN conduction in IGN branching axons is facilitated following 5 and 10 Hz stimulation (n=3). No changes were seen in unbranching axons of the splanchnic nerve. **(B)** Response amplitude but not frequency-dependent depression is altered following block of the α3 Na-K pump. Shown is the amplitude of evoked responses in the T4 caudal IGN to stimulation of the IGN rostral to the T4 ganglion. Several episodes of 10 pulse trains were delivered at 20 Hz with either 30sec or 5sec interburst interval. Frequency dependent depression was seen at 5sec interburst interval. Low dose Ouabain (0.5 μM) greatly reduced spike amplitude but not frequency dependent depression.

Cl^- transporters are also under circadian control via circadian variation in mTOR [36]. Activation of this kinase can be associated with activation of the WNK-SPAK pathway that reciprocally regulates these two Cl^- transporters, promoting increased intracellular chloride [36]. The hypothalamic suprachiasmatic nucleus (**SCN**) contains the master biological clock and differential activity in KCC2 and NKCC1 drives circadian variation in GABAergic synaptic transmission in different neuron populations in the SCN, with variation that appears largely due to regulation of KCC2 [81]. The SCN also projects to neurons in two other hypothalamic nuclei with direct projections to spinal cord SPNs [82] that may indirectly drive SPN excitability changes via activity-dependent neuropeptide release. SPNs themselves may have intrinsic circadian variability in KCC2 and NKCC1 function, as the expression levels of clock genes PER2 and BMAL1 broadly correlate with the expression of mTOR in an RNAseq study of gene expression in SPNs [47]. Thus, there may be circadian variation in the modulatory role of constitutively active $GABA_AR$s in spike conduction along SPN axons. Preliminary insight can be provided from modeling studies as shown below. We have yet to test the effects of transport blockers on function. Previously, the NKCC1 antagonist bumetanide was shown to decrease pain after SCI in both animal models [19] and clinically [83], presumably via increasing inhibitory $GABA_AR$ function by reducing intracellular Cl^- to hyperpolarize E_{Cl}. **(e) Neuromodulation.** A notable prominent feature of homeostasis is the need for a variable setpoint controller with input-output regulatable feedback control [84] to operate over an adjustable range influenced by physio-behavioral states (rest, arousal states, exploratory behaviors requiring locomotion, sleep stage). Neuropeptides present powerful neuromodulators known to affect behavioral state [85, 86]. The abundance of neuromodulatory transmitters and receptors is a unique defining feature of SPN populations [47, 87] and may help provide for an adjustable output. The neuropeptide CART is involved in modulation of energy balance [88, 89]. CART is present in several transcriptionally-identified classes of SPN neurons [47]. $CART^+$ SPN neurons receive input from brainstem pathways controlling muscle and skin vasoconstrictors and project exclusively to NPY^+ vasculature-innervating postganglionic neurons and account for ~70% of their total synaptic input [59].

SIGNIFICANCE. Combined approaches will provide unprecedented experimental insights that will deepen and transform our understanding of the role of modifiable conduction across SPN branching axons in the CNS-PNS control of this homeostatic circuit. Insights derived from probing the network parameter space could greatly hasten discovery of putative neural bases of various

aspects of autonomic dysfunction and catalyze use for drug discovery-based simulations that inform new therapeutic approaches.

METHODOLOGICAL. Novelty of approach. Despite the complexity in organization and potential to be a site of modulation, SPN-to-postganglionic neurons thoracic connections are rarely studied perhaps due to technical challenges [45, 48]. The adult mouse *ex vivo* preparation provides access to study SPN rostro-caudal axonal conduction across many sympathetic chain ganglia for electrophysiological, opto- & chemo-genetics and pharmacology studies in a bath chamber with T° control. **CONCEPTUAL. (1)** Branch points may represent a locus for shaping sympathetic gain. Sympathetic response magnitude in sympathetic chain postganglionic neurons across the CNS-PNS interface is thought to be regulated by ①SPN firing and strength of ②synaptic transmission. Studies leveraged by preliminary data support a broadening of our conceptual understanding of mechanisms of gain control to include conduction control across branch points as a ③third major control site. One primary function may be to control spatial selectivity of sympathetic drive. **(2)** Ignored role for modulation via $GABA_ARs$. Constitutively active α_5-$GABA_ARs$ are known to modulate activity of spinal SPN cell bodies [70]. We test the hypothesis that their expression and modulation in SPN axons provides a novel fundamental site of CNS-PNS output control. In addition other α_5-$GABA_ARs$ have nM GABA sensitivity [70] and GABA has long been known to act as a peripheral hormone/neuromodulator [69, 90]. As SPN axons are exposed to interstitial fluid $GABA_ARs$ may be modulated by low circulating plasma GABA. Intriguingly, $GABA_ARs$ are exquisitely controlled by numerous allosteric modulators [91] including systemic neurosteroids and proinflammatory cytokines [31-35]. For example, stress-related production of 3α-reduced neuroactive steroids could function to control sympathetic output strength as potent positive allosteric modulators of α_5-$GABA_ARs$ [31-34]. Patients with panic disorder have increased plasma concentrations of 3α-reduced neuroactive steroids [92]. Conversely, IL-6 and TNF-α may reduce $GABA_AR$ activity via receptor internalization [35]. **(3)** Role of T° changes in altering spike conduction across branch points. The consequence of body T° fluctuations on SPN axonal function beyond the normal physiological range has yet to be explored. As $T°_{core}$ operates within a narrow range, broader T° fluctuations seen in SCI patients may functionally impact sympathetic signal amplification. Whether moderate $\uparrow T°_{core}$ or $\downarrow T°_{core}$ contribute incidents of SCI-induced autonomic dysfunction is unknown but may be clinically relevant. **(4)** Possible site of plasticity after SCI. Injury and disease have been shown to increase susceptibility to conduction block of neurons in general but the extent to which it contributes to various dysautonomias remains a completely unexplored field of study [49, 93]. Understanding alterations in their activity in disease, particularly after SCI, may contribute to a broader picture of dysfunction in vascular perfusion control and thermoregulation [24-27]. **THERAPEUTICS. (1)** Pharmacology. The overlooked role of $GABA_ARs$ and their possible control by humoral endogenous allosteric modulators may transform our understanding of autonomic gain control at the CNS-PNS interface and introduce α_5-$GABA_ARs$ as a novel pharmacologic target for the management of dysautonomias. **(2)** Electrotherapeutics. Control of branch point excitability may be amenable to long-lasting electrotherapeutic neuromodulatory control, including via DC stimulation [62, 94].

3. METHODS & PRELIMINARY DATA

GENERAL METHODS. C57BL/6 backcrossed ChAT-CHR2 or CART-CHR2 transgenic adult mice (2-4 months old) of both sexes are used and include control, acute-SCI (1-3 days) and chronic-SCI (4-6 weeks) populations. The T2 level was chosen so ensure experimental animals develop robust autonomic dysfunction and are prone to hypo- and hyperthermia [95, 96]. Post-surgical time points

were selected to allow for data collection during periods of neurogenic shock [97-99] and inflammation [100-102] (acute) and autonomic dysfunction (chronic) [103, 104]. Proposed studies are undertaken at 22-40°C (35-37°C is common thermoneutral range in mice [105]). In humans hypo- and hyperthermia values are <35°C [25] and >38°C [30, 106, 107]. **The *ex vivo* thoracic paravertebral sympathetic chain preparation (*Fig 2*).** Specialty fabricated, 'hourglass'-shaped, tight fitting glass suction electrodes are used for stimulation and recording to assure stable recordings [48]. Stimulating electrodes are placed on ventral roots to recruit preganglionic axons from each thoracic spinal segment. A Peltier device provides temperature control of the bath chamber. Drugs are applied at known concentration via bath superfusion. This preparation overcomes limitations in accessibility [48]. It has intact connections from ventral roots and enables multisegmental assessment of SPN conduction using electrical and optogenetic stimulation. **Comparing spike propagation along chain ganglia to propagation along splanchnic nerve (*Fig 2B*)**. The experimental arrangements are as shown or are derivative to that shown. The splanchnic nerve is cut such that its length is homologous to the IGN. Adjacent ventral roots (T7-T9 or T10-T12) are serially stimulated while recording from the rostral-T6 IGN, caudal-T10 IGN and splanchnic nerve. Recording electrodes are placed on cut ends of the IGN and splanchnic. Stimulation of ventral roots at increasing distances from the segment recorded will serve as a proxy for increasing number of branch points. In the same or separate experiments, progressive placement of fiberoptic blue light illumination along the IGN or at the ventral root will assess sensitivity to block across increasing number of branch points. **Separating direct from synaptically evoked spiking responses (*Fig 2C*).** As evoked spiking may include synaptically-activated postganglionic neurons, studies are undertaken following block of SPN nicotinic acetylcholine receptor (**nAChR**) synaptic actions with hexamethonium (100μM) which acts on postganglionic $\alpha_3\beta_4$ nAChRs [108]. While not used in preliminary experiments above, atropine (10μM) is now commonly applied to prevent muscarinic receptor-mediated actions on postganglionic neurons [109]. **Recruitment of SPN axons.** (*Fig 2B&C*). This is achieved by electrical or optogenetic stimulation of thoracic ventral roots or optogenetic stimulation of the interganglionic nerve (**IGN**). Myelinated and unmyelinated SPN populations can be differentiated by the stimulation intensity required for recruitment and by conduction velocity (not shown). Electrical stimulation is undertaken at >2x supramaximal stimulation intensity (typically 200μA, 200μs) to ensure that observed drug or T° changes are not due to threshold excitability differences in the composition of recruited axons (*Fig 4*). Supramaximal optical stimulation may not be possible and may instead be undertaken at 5x threshold (**T**). Distance between stimulation and recording electrodes are measured to allow calculation of axonal conduction velocities (as we have done in a preliminary report [23] - not shown).

PRELIMINARY DATA. CNS preganglionic projections issue complex multisegmental branching patterns into thoracic chain ganglia (*Figs 2D&3*). SPNs issue axonal projections onto paravertebral sympathetic chain postganglionic neurons via the ventral root, then through the white ramus and are predominantly unmyelinated [37]. We used Neurobiotin orthograde axonal labeling via cut SPN axons in ventral roots to obtain important anatomical insight into SPN divergence and organizational features of branching. SPN primary axons form T-shaped branches with daughter axons traveling rostrocaudally to form synaptic connections across many ganglia. Shown is how they collateralize within ganglia to innervate postganglionic neurons then coalesce for subsequent travel to the next ganglion via the interganglionic nerve (**IGN**). **Branching axons are preferentially sensitive to T°-dependent changes in conduction.** (*Fig 5A*). Conduction failures may be a feature of low safety factor conduction across branch points. This was seen as a reduction

of identifiable individual events and/or as a decrease in the amplitude of the population response (***Fig 4***) and can be quantified by integrating the rectified response When examined at 31-36^{0}C spontaneous time-dependent conduction block was always seen across ≥ 3 intervening ganglia (n=6/6) but never across ≤2 segments (n=0/2). **Evidence of constitutively active α5-GABA$_A$Rs in modulating SPN axonal conduction and response plasticity after SCI (*Fig 6A*).** The α5-GABA$_A$R inverse agonist L655, 708 increased conduction across branching axons in uninjured mice, with opposite conduction blocking actions in mice having undergone T2 spinal transection ≥ 3 weeks prior. Results strongly support a role for constitutively active α$_5$-GABA$_A$Rs in control of axonal conduction [13, 70, 110]. The observation of a switching in the functional role of the α5-GABA$_A$Rs after SCI suggest that the physiological range of gain control and rostrocaudal influence could be dramatic. One possibility is that constitutively active GABA$_A$Rs are now facilitating conduction based on depolarized E_{Cl} which is then inhibited by L655,708. This is consistent with our knowledge that after SCI there is a reduced functioning of KCC2 in CNS neurons, presumably including SPNs [21, 22]. **Circadian difference in excitability (*Fig 6B*).** SPNs may have circadian variation as part of broader physiological control systems that may associate with mTOR related signaling actions on Cl- transporters in protein synthesis [36]. One prediction is that changes are associated animals transitioning to a waking state. We mined data from a separate ongoing study that captured spontaneous SPN synaptic activity in postganglionic neurons over an experiment period that overlapped the transition between day and night in mice (6PM). We observed a moderate but significant correlation. This does not link directly to a role for changes in E_{Cl}, but is consistent with this possibility and will be explored in this project. Periods of more depolarized E_{Cl} would support increased propagation across branch points in a form of gain control. Importantly, modeling efforts as described below can provide insight into how modulation of excitability through GABA$_A$Rs can affect output gain to reflect physiological status in this circuit.

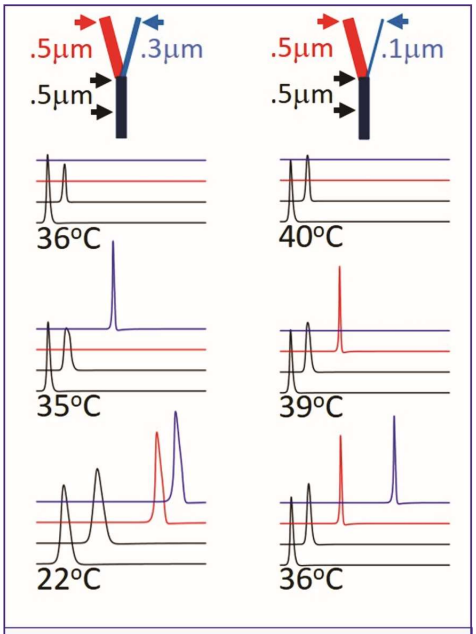

Figure 8. Influence of T ° on branch point failure. Two model configurations (top) differ only in D2 diameter (blue). Voltage traces (bottom) show membrane potential at different T °s for the locations indicated by arrows at top. Both model versions show a transition from no failure, to one branch failing, to both branches failing, as T°increases. In the left model the wider branch fails first, while in the right model the narrower branch fails first as T°increases.

Branching axons are preferentially sensitive to frequency dependent changes in conduction (*Fig 7A*). At a physiologically relevant T° (36ºC) we observed consistent frequency dependent facilitation of evoked responses in branched SPN axons but not in non-branching axons (n=3). **Ouabain had no effect on frequency dependent depression** (***Fig 7B***). We also assessed evidence that α3-containing Na-K pumps, expressed in all neurons and thought to reflect spiking history, are altered following it pump block with ouabain [61, 111]. We found that ouabain had no effect on frequency dependent depression but reduced the amplitude of the evoked response. This is not consistent with preferential recruitment of the α3 Na-K pump but is consistent with partial bock of the pump reducing Na^+ extrusion. Additional studies are required to determine whether these effects are temperature- and/or time-of-day dependent and if altered after SCI.

PRELIMINARY MODELING STUDIES. We have constructed a preliminary conductance-based model of an axonal branch point at which a parent axon P branches into two daughter axons D_1 and D_2. The model is implemented in Python code using integration method by Hines [112]. In its prototype stage the model contains four membrane currents – fast sodium I_{Na}, delayed rectifier I_{Kd}, leak, and I_{GABA} to represent $GABA_A$ receptor mediated chloride flux. Parameters of I_{Na} and I_{Kd} are adapted from our model of postganglionic neurons [45]. Temperature is modeled through its influence on ionic reversal potentials via the Nernst equation and on ion channel gating time constants using a Q10 = 3, typical for channels [113].

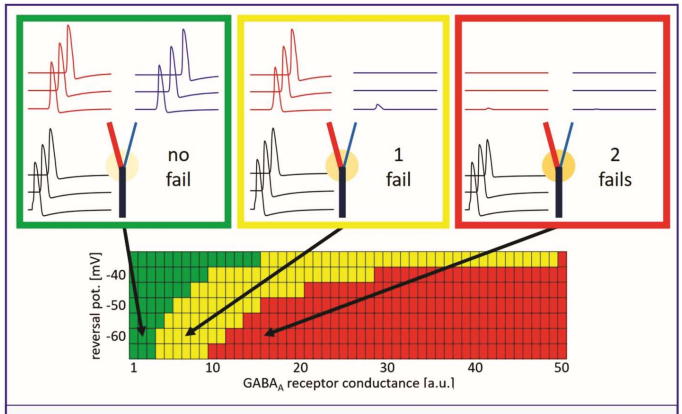

Figure 9. Effect of g_{GABA} and on branch point failure. Top, simulated action potential propagation in a branching axon E_{Cl} with low (left), intermediate (middle), and high (right) gGABA in axon segments near the branch point. Voltage traces correspond to the middle and ends of the P (black), D1 (red), and D2 (blue). A spike initiated in P invades both D1 and D2 for small g_{GABA}, only D1 for intermediate, and neither branch for large gGABA. Bottom, dependence of branch point failure on g_{GABA} and E_{Cl}. Green – no branch point failure, yellow - one branch fails, red – both branches fail.

Figs 8 & 9 show model pilot studies on the effect of axon and branch point geometry, T° and $GABA_A$Rs, on branch point failure. **Effect of T° changes.** In ***Fig 8***, the model is used in two configurations identical except for the diameter of D_2 – 0.3µm (left) vs. 0.1µm (right) – to investigate the effect of T°. P, D_1, and D_2 are 1mm long and a spike is initiated in P. As T° is increased, both model versions exhibit a transition from faithful spike propagation in D_1 and D_2, to failure in one branch, to failure in both. In the model at left (0.3µm D_2), this transition occurs between the T° frequently used in experiments (22°C) including the electrophysiological studies in the sympathetic chain that assessed magnitude of SPN divergence and assumption that propagation occurs without fail [2-7], and mouse body T° (36°C), emphasizing the importance of T° as an experimental parameter. In the model at right, spikes propagate without failure at normal body T° and below, but begin to fail at higher T°, indicating one way in which fever or hyperthermia can affect sympathetic and other neural system function. Interestingly, in the left model the wider D_1 (red) fails first as T° increases, while at right, the narrower D_1 (blue) fails first. This indicates two different failure mechanisms that can be explained by interactions between axon geometry and T°-dependent spike duration [36]. **Effect of E_{Cl} and $GABA_A$R conductance changes.** ***Fig 9*** shows how $GABA_A$Rs and E_{Cl} could control branch point failure. The model was configured with lengths of 1mm for P, D_1 and D_2, and diameters of 0.5µm (P), 0.4µm (D_1), and 0.2µm (D_2). All three axons (P, D_1, and D_2) contain $GABA_A$Rs (modeled as aCl^- conductance g_{GABA}) in a 10µm long axon segment adjacent to the branch point, but not at the branch point itself or in the rest of the axon, inspired by [114]. When a spike is elicited at the far end of P, it propagates to the branch point and invades both D_1 and D_2, only the (wider) D_1, or neither, depending on the magnitude of g_{GABA} and E_{Cl}, with failures more likely for larger g_{GABA} and more hyperpolarized E_{Cl}. This supports our hypothesis that $GABA_A$ receptors near axonal branch points provide a potential avenue for modulatory control of signal propagation in the sympathetic nervous system. Notably, the figure includes a range of g_{GABA} (10 – 16 a.u.) over which changes in E_{Cl} – such as might occur because of circadian [36] or SCI injury-induced [21, 22] changes in ion transporter expression – could alter autonomic function.

4. EXPERIMENTAL AND MODELING METHODS AND RESEARCH STRATEGIES

Overview. The central hypothesis in this proposal is that signal propagation across highly divergent SPN axons is not hard-wired, but rather physiologically modifiable at branch points. Specific aims proposed. **[SA1]** tests whether conduction across SPN branch points is influenced by T° across the physiological range of hypo- and hyperthermia, and also associated with thermoregulatory dysfunction in high injury SCI. **[SA2]** tests whether conduction across SPN branch points is under neuromodulatory control by $GABA_AR$s, which may be modulated reciprocally controlled Cl^- transporters that regulate E_{Cl}, which is modulated by signal transduction pathways from various neuromodulators including those strongly associated with circadian variation in protein synthesis by mTOR, and which is altered after SCI. **[SA3]** will test whether spike propagation is activity dependent including by the highly Na^+-sensitive α3 NA-K pump thought to serve as a rheostat for activation history. **[SA4]** will undertake essential computational modeling studies that support experimental observations as well as provide predictive insight into subsequent studies and mechanisms of action with focus on T°, effects of $GABA_AR$ conductance and various locations including branch points and effects of ECL on these conductances.

We will test for control of spike conduction across branch points in the highly divergent SPN projections across the paravertebral sympathetic chain in comparison to nonbranching axons that project to prevertebral ganglia. Studies on SPNs will be undertaken with electrical and optical (ChAT-CHR2 and CART-CHR2 mice) stimulation-based recruitment of SPNs.

[SA1] Conduction across SPN branch points is T^0-sensitive.

Hypothesis. Spike propagation across SPN branch points is T°-sensitive and altered by hypo- and hyperthermia. **Rationale.** Conduction failures become more common as T° elevates [8, 9, 49]. The mechanism by which high T° elicits conduction failures is probably by reducing the width and amplitude of the spike [8]. SPNs are largely unmyelinated (Fig 2b) and thus are expected to be very sensitive to conduction block at elevated T° [9]. Lower safety factor at axonal branch points may increase likelihood of T°-sensitive conduction block [52-54] and these results are supported by initial comparison with unbranching axons (***Fig 5***). **Methods.** Experimental approach is as described in General Methods. Starting at 36°C, a command controlled Peltier device will mimic hypothermic conditions by reducing bath T° down to 30°C [29] and hyperthermic conditions by increasing bath T° up to 40°C [115]. Conduction changes will be assessed in 0.5° changes in T°. To assess conduction changes we will normalize elevated and reduced T° response to those captured at 36°C. **Interpreting Outcomes and Alternative Approaches**. **(a)** Hyperthermic conditions should block conduction while hypothermic conditions should facilitate it. **(b)** Branching SPNs should be more sensitive conduction block at elevated T°. Even small elevations above $T°_{core}$ should compromise spike conduction across branch points (***Fig 8***) [9].

[SA2] Conduction across SPN branch points is under neuromodulatory control of $GABA_A$ Rs.

Hypothesis. Spike propagation across SPN branch points is regulated physiologically by modulation of axonal $GABA_AR$s that may include constitutively active and GABARs with low sensitivity to GABA. Examination of conductance differences will be assessed across various T°, after SCI, following block of NKCC1 or KCC2 transport, and at different times of day. **Rationale.** *[For details rationale see the Significance section (c) Extrasynaptic $GABA_ARs$]* **Methods.** We begin at 36°C. We will electrically or optogenetically recruit SPN axons across interposed chain segments while recording population responses in branching and unbranching SPNs. Axonal

recruitment will be assessed following application of $GABA_AR$ agonists, antagonists, inverse agonists and endogenous neurosteroid allosteric modulators [2, 44]. Drugs are applied and changes in conduction assessed at low frequencies to provide reproducible response between trials (e.g. 1/30s). Drug dosage will be based on studies showing full block in more intact ex-vivo systems that are studied *in vitro* or at doses at 10x the reported EC50/(Kd) or IC_{50} (Ki) values determined in cell assay systems [91]. For drugs showing pharmacological actions, doses will be applied at increasing levels to construct cumulative dose-response curves. Regarding α_5-containing $GABA_A$ receptors, bicuculline, picrotoxin (channel blocker) and perhaps gabazine are antagonists. DMCM and L-655,708 are high affinity inverse agonists, muscimol and isoguvacine are full agonists, and there are an abundance of allosteric modulators listed at the IUPHAR/BPS guide to pharmacology website [116]. We will also test neurosteroids (tetrahydrodeoxycorticosterone [THDOC], pregnanolone [3α,5β-THP], and zuranalone) and basmisanil as a highly selective α_5-$GABA_A$ negative allosteric modulator [116] to obtain insight into potential endocrine modes of modulation. To assess the role of Cl^- transporters we will apply the NKCC1 antagonist bumetanide (5mM) [83] and the KCC2 antagonists VU0240551 (50 μM) [81] and VU0463271 (1 μM) [117]. We will also undertake experiments staggered to overlap with transitions from active to inactive and inactive to active periods. **Interpreting Outcomes and Alternative Approaches.** **(a)** $GABA_ARs$. If α_5-$GABA_ARs$ are constitutively active with hyperpolarizing E_{Cl} (expected of CNS neurons like SPNs) we would predict; α_5-$GABA_AR$ inverse agonists to increase conduction across branch points, full agonists to have little action, positive allosteric modulators to also depress, and negative allosteric modulators to facilitate actions. If $GABA_AR$ actions are at branch points but also in unbranching axons, antagonists for $GABA_ARs$ may have a different profile of that may indicate different subunit composition. If modulatory actions are seeing but do not differ between branching IGN and unbranching splanchnic SPNs, we would conclude that $GABA_ARs$ allow for flexible control of SPN signaling by mechanisms independent of branch points. In this case modeling studies will be modified to assess distributed distributions of $GABA_ARs$. Note, that for the case of branching axons we cannot exclude the possibility that spread and magnitude of amplification may still be a consequence of changes independent of safety factor across branch points because we cannot undertake interactional recordings. This is where will be important to obtain insight from modeling studies. Immunohistochemical studies on receptor location would provide strongly support necessity [13]. **(b)** Branch points. We expect the degree of facilitation or block to increase with distance between recording and stimulating sites in branching SPNs based on number of branch points. **(c)** Capturing individual rather than population responses to interpret conduction block. While we can confidently assess conduction block in the far fewer myelinated axons (***Fig 4***), supramaximal axon recruitment limits ability to characterize individual units in the much more numerous and variably conducting unmyelinated axons (see ***Figs 2&4***). The high variability seen suggests that unmyelinated axon propagation across branch points has low safety factor. We chose not to grade stimulus intensity to exclude the possibility of recruitment changes being due to drug or Tº axonal polarization induced changes threshold for recruitment [see next section]. One method that may help assess activation/failures in individual unmyelinated SPNs involves preferential recruitment of unmyelinated SPNs. As optogenetic activation preferentially recruits slowest-conducting fibers first (not shown), we will attempt to identify individual axons at low threshold illumination intensities [118]. **(d)** Other factors controlling safety factor at branch points. In the absence-of or in-addition-to $GABA_AR$ modulation, we may explore a role for other implicated channels including; Cav3.2 Ca^{2+} (block with mibefradil)[50] and voltage-gated K^+

channel blockers known to reduce spike propagation failures (e.g. 4-AP, TEA). Results will help compare mouse to historical studies in cervical & lumbar ganglia in larger mammals [119].

[SA1&2] Determine whether T° & $GABA_AR$ sensitivity is altered after SCI and tome of day.

Hypothesis. High thoracic SCI leads to; **(a)** increased $GABA_AR$ activity that promotes branch point conduction, and **(b)** spike width broadening to further promote conduction and reduce the impact of elevations above $T°_{core}$. **Rationale.** Injury-induced plasticity in SPNs may be central to the emergence of circuit dysfunction. Broader T° fluctuations seen in SCI patients, may functionally impact sympathetic signal amplification [24-27]. Increased $GABA_AR$ constitutive activity may limit conduction block. **Methods.** Experimental approach is as in General Methods and [SA1] starting at 35°C. We will compare results obtained in **[SA 1 & 2]** to responses seen in mice after acute (3-5 days), and chronic T2-SCI (4-6 weeks). Experiments on $GABA_ARs$ and T° will be streamlined to most salient effects observed in **[SA 1 & 2]** to minimize sample and ensure both $GABA_AR$ and T° results are obtained in each animal. Studies will focus on use of the inverse agonist L-655,708, given the success of our initial experiments.

[SA3] Activity-dependent changes in conduction.

Hypotheses. **(a)** Conduction across branch points undergoes frequency dependent facilitation following short trains (5-20 Hz) whereas no change will be seen in nonbranching axons. **(b)** Prolonged high frequency stimulation at these frequencies will instead reduce conduction velocity with persistent depression of population amplitude. This activity is modulated by axonal α3 Na-K pump activity. **(c)** A genetically distinct subpopulation of SPNs expressing CART, may be resistant to frequency dependent depression. **Rationale.** Recruitment of SPNs is driven predominantly by descending drive systems with persistent actions over long periods at low frequency, however, higher frequencies are also seen during excessive physiological stress and may associate with CART-expressing SPNs. We will use selective optogenetic activation in CART-CHR2 SPNs to see if there is differential sensitivity to frequency dependent changes. **Methods.** We will deliver stimuli at increasing frequencies (0.1, 1, 5, 10, and 50 Hz) electrically as well as optogenetically to assess frequency dependent features of spike conduction. The α_3 NA-K pump. We will assess the role of the α_3 NA-K pump in controlling firing in SPN axons through pharmacological inhibition (ouabain [0.5 μM]), or activation (monensin [10 μM]). While we expected low dose ouabain block of the SPN axonal α3 Na-K pump to limit frequency-dependent spiking, we instead observed reduced population spike amplitudes, perhaps due to axonal depolarization by compromised Na^+ extrusion (***Fig 7B***). **Interpreting Outcomes and Alternative Approaches.** **(a)** Stimulation frequency. We expect that myelinated SPNs more easily conduct across branch points and that unmyelinated SPN conduction is preferentially sensitive to modulation by stimulation frequency. **(b)** Unlike unmyelinated afferents, high frequency stimulation may facilitate recruitment of myelinated and CART-expressing axons [59, 60, 109].

Anatomical and physiological characterization of branch points to inform modeling studies.

Anatomical studies will help inform modeling simulations by providing counts of SPN axons, projection distances, branching and axon diameters. (i) Neurobiotin labeling. Preliminary effort succeeded in labeling and permitting counting of axons (***Fig 3***). Neurobiotin (5% W:V) is filled into suction electrodes (~70μm diameter) attached to an exposed ventral root and left for 6 hours at room temperature. Due to the effort required for the studies we will focus exclusively on SPNs arising from T7 ventral root, though individual comparisons to a couple different thoracic segments will also be undertaken, time permitting. Fluorescence labeling is provided by processing

with Extravidin FITC (1:500) with dissected intact chains coverslippe for microscopic imaging by by Confocal Microscopy (Olympus FV1000, 100x, NA1.45) and counted manually in FIJI/ImageJ2 software. Working with Emory's imaging core (ICI) we have determined the limits of reliable axon diameter captured with high-resolution confocal microscopic to be ~300 nm. This is insufficient for diameter estimation, but sufficient to accurately visualize retracing and quantification of projections. s (ii) Axon diameters estimates. Initial modeling of axon diameters has relied on lectron microscopic (EM) measures from a more rostral cervical sympathetic ganglion [37]. While a similar range of values is likely in the thoracic sympathetic chain, measure this to further affirm modeling. We will provide multiple segments of thoracic chain ganglia to the EM core for axon size estimation. (iii) Conduction velocity. While myelinated neuron axonal conduction velocity varies linearly with diameter, ($CV \propto d$), unmyelinated axon conduction velocity varies as the square root ($CV \propto \sqrt{d}$) [120]. By estimating conduction velocity across progressively distant individual ganglia we will obtain a relative appreciation of distant dependent changes in axon diameter. Initial studies observed reductions down to 0.2 m/s [23].

[SA4] To examine interacting factors controlling autonomic axonal conduction.

Hypothesis. Autonomic CNS-PNS signaling is modulatable through physiological control of SPN axon and branch point properties. **Rationale.** Many factors (**F**) influence the propagation of SPN signals to postganglionic neurons, including T°, $GABA_AR$ modulation, axon geometry, biophysical properties, circadian changes in transporters, and prior electrical activity via pump activation. Some of these F, including $GABA_AR$ activation **[SA1]** and temperature **[SA2]**, can be varied experimentally and their effect on SPN axonal signaling examined with extracellular recordings (as the small axon diameters prohibit intracellular recording). Other F, such as geometry, are not manipulatable. Furthermore, as ***Fig 8*** illustrates, F can interact in counter-intuitive ways – why does the narrower branch fail before the wider branch in one model, but after it in the other, as T° increases? Yet the large number of F that control SPN signaling to the sympathetic chain makes full experimental investigation of their interactions prohibitively laborious. For these reasons we will complement our experiments with a comprehensive ensemble model of signal conduction in branching SPN axons. **Methods. (i)** We will construct a model of branching axonal projections from SPNs and use it to examine how T°, $GABA_AR$ modulation, axon geometry, biophysical properties, transporters, and activity interact to shape sympathetic signaling. The prototype model described in the Preliminary Data section is a multi-compartment model of an axonal branch point four membrane currents – a fast sodium current I_{Na}, a delayed rectifier current I_{Kd}, a leak current, and a chloride current I_{GABA}, with parameters of I_{Na} and I_{Kd} adapted from our mouse sympathetic postganglionic neuron model [45]. T° is modeled through its influence on ionic reversal potentials via the Nernst equation, and on ion channel gating time constants using a generic Q10 = 3 [113]. **(ii)** To extend this model we will 1) include additional Na^+, K^+, Ca^{2+}, and Cl^- currents based on SPN ion channel expression profiles [47], 2) insert chloride transporters (KCC2 and NKCC1) and Na-K pump, 3) create dynamic variables for intracellular K^+ and Na^+ concentration (to reflect pump activity), Ca^{2+} (to control activation of Ca^{2+}-dependent K^+ conductance), and Cl^- (to reflect Cl^- transporter activity and Cl^- flux due to $GABA_AR$) and the respective reversal potentials, 4) where available, analyze data from literature and our own experiments to constrain ion channel, pump, and transporter parameters, including Q10s, and axial resistivity. This will unavoidably leave many parameters unconstrained, as SPN axonal properties are uncharacterized, so we will 5) tune under-constrained parameters to match existing recordings from SPN axons and new data generated in **[SA 1 – 3]**. Regarding axon geometry, we will 6) expand the model architecture to include secondary and tertiary branch points

and synaptic boutons, and 7) modify the model to allow for diameter variations along each axon section, for example to accommodate tapering axon diameter. Finally, we will 8) obtain estimates for axon diameter and length distributions and relationships between parent and daughter branch diameters from existing (***Figs 2, 3***) and new data and apply ensemble modeling [121]: we will generate an ensemble (**E**) of model versions (on the order of a hundreds) whose geometric distributions (diameters, lengths of axons sections, number and location of branch points, relationship between pre- and post-branch diameters) reflect biological inter-individual variability. Using the ensemble E constructed in this manner, we will then examine factors F that potentially influence failure of action potential propagation through branching SPN axons, and thus the spatial distribution of SPN signaling to the sympathetic chain ganglia. These F include: magnitude and distribution of $GABA_AR$ mediated Cl^- conductance along the axon and especially near branch points, magnitude of transporter and pump mechanisms, maximal ionic membrane conductances, T^o, and frequency of SPN spiking (to investigate activity-dependence of failure). Each F will at first be varied individually to determine whether, in which direction, and how much it influences SPN signaling. This will be assessed by simulating all model versions in E while varying F. For each model version we will determine what fraction **S** (for "safety") of terminal ends of the branching axon is reached by the propagating spike, with S = 1 indicating that no branch point failures occurred at any primary, secondary, or tertiary branch points, and S < 1 meaning that a propagation failure occurred somewhere along the way from spike initiation in P to one or several terminal points. At the ensemble level, we will ask how varying F shapes the distribution of S values across E. If F is $GABA_AR$ activation or T^o, this analysis will directly relate to **[SA1 & 2]**.

Beyond this quantitative assessment of the influence of F on S across E, we will analyze a sample of model versions that exhibit failures by looking at simulated voltage and current traces proximal and distal to the failing branch point to gain insight into the mechanism(s) of failure.To learn about interactions between factors, we will execute 2D parameter sweeps analogous to that in ***Fig 9*** by varying two factors F_1 and F_2 simultaneously and determining the distribution of S values across E for various combinations of F_1 and F_2 values. In particular, this will be instructive for $GABA_AR$ activation and T^o as factors F_1 and F_2, as it will allow us to determine whether any changes in $GABA_AR$ and/or T^o sensitivity after SCI (as studied in **[SA3]**) are in a compensatory direction, and whether they act synergistically or counteract each other. **Interpreting Outcomes and Alternative Approaches.** We expect that $GABA_AR$ levels, but also Cl^- transporter activity through its effect on E_{Cl}, and potentially other factors F, will prove to be potent regulators of S, and thus suitable targets for modulatory control of autonomic function. If any F shows strong interaction with T^o in our 2D sweeps, it would implicate F as a potential avenue for compensatory physiological changes to cope with T^o dysregulation after SCI.

5. Broader Impacts of the Proposed Work

1. Research-related. Ensemble modeling will provide mechanistic insights beyond experiments. This is time and resource effective, and reduces number of animals needed. **Prinz.** Prinz has a track record in computational neuroscience. Applying her experience to the under-studied sympathetic nervous system synergizes with the proposed experiments. **Hochman.** Hochman has a long history of studies on spinal systems. This allows him to initiate rigorous studies on changes in autonomic function after SCI. **2. Societal impact. Prinz** has a record of mentoring women – 3 of 6 grad, and URMs. She fosters educational and outreach activities in her mentees. Her research in the lab involves (currently 3, 1 URM). **Hochman** has been PhD adviser to 6 women in BME; a current BME PhD student is a female URM student funded via NSF GRFP. He mentors at all levels, led the creation of a 'green paper' on bias, and created a workshop on bias for NS students.

6. COORDINATION PLAN

The expertise of the PIs is well fitted to examine modulatability of autonomic function at the CNS-PNS interface. Collectively, the investigators undertake difficult approaches across an underappreciated domain of inquiry. Hochman (in Cell Biology) has deep understanding of spinal segmental integrative actions. Prinz is a world leader in computational modeling of neurons. Their labs are located in adjacent, connected buildings. Studies on modulation and control of cellular signaling feed into their strengths.

1) Specific roles of the collaborating PIs and other Senior Personnel.

(a) Shawn Hochman will be directly responsible for supervising progress in all the electrophysiology and anatomy experiments undertaken. He will have weekly one-hour meetings with each individual independently, will participate in some of the experiments, and will be directly involved in participating with data analysis and writing of manuscripts.

(b) Astrid Prinz will be directly responsible for supervising progress in all computational modeling approaches. She will have weekly one-hour meetings with each individual independently, and will ensure that sufficient information exchange occurs between experiments undertaken in the Hochman lab and results obtained to best synergize with computational approaches. She will be directly involved in participating with model design and execution, data analysis and writing of manuscripts.

(c) Authorship order will be discussed among PIs and any conflicts of opinion will be adjudicated by an impartial third party.

2) How the project will be managed across disciplines.

Information exchange will occur at three interaction levels. The PIs will meet monthly to discuss general research strategy moving forward. All involved individuals in both laboratories will also meet monthly to update progress, for cross-fertilization of ideas and insights moving forward, and to present data in a mini-symposium format. They will also invite other local experts within their respective domains of expertise to help assess progress and ensure sufficient information exchange across disciplines.

3) Identification of the specific coordination mechanisms that will enable cross-discipline scientific integration.

Both PIs will attend and require students and postdocs to attend an integrative neuroscience seminar series run by Hochman that involves presentations from faculty, students and postdocs within the integrative neuroscience domain of expertise, which includes biomedical engineers from Georgia Tech, human research scientists from rehab medicine, computational neuroscientists predominantly from the Department of Biology, and spinal cord electrophysiologist predominantly from the Department of Cell Biology.

4) Specific references to the budget line items that support these coordination mechanisms.

As the collaborating PIs are at the same institution with labs in adjacent connected buildings, there are no specific budget line items explicitly required to support coordinating mechanisms.

5) Results from prior and current support from CRCNS-participating organizations (past 5 years).

Hochman and Prinz: NIH R01NS102871: Recruitment principles and injury-induced plasticity in thoracic paravertebral sympathetic postganglionic neurons

7/1/17 - 6/30/22; $218,750 (direct)

This project is characterizing the properties of thoracic chain ganglia and incorporates computational modeling to investigate principles of their operation as well as their plasticity after SCI. Data and code from this project will be shared via Academic Torrents, GitHub, and ModelDB.

Hochman: NIH R21NS116724: Modifiability of conduction across preganglionic axonal branch points
5/1/21- 10/31/22; $275,000 (direct)
This exploratory study is laying the groundwork for the present proposal by testing for regulation of conduction by extrasynaptic $GABA_A$ receptors and T^o shifts and has resulted in some of the initial evidence motivating the present proposal. In contrast to the present proposal it does not address possible circadian variation in autonomic function and activity-dependent changes in conduction via the Na-K pump, and does not include a computational component. Data from this project will be shared via Academic Torrents and/or the CRCNS data sharing infrastructure.